

## Research Paper

## Sound Radiation Characteristics of Acoustically Thick Composite Cylinders and Their Experimental Verification

S. JOSEPHINE KELVINA FLORENCE<sup>(1)\*</sup>, K. RENJI<sup>(2)</sup><sup>(1)</sup> Structures Group, U. R. Rao Satellite Centre  
Bangalore, India-560017

\*Corresponding Author e-mail: florajosephine2000@gmail.com

<sup>(2)</sup> Advanced Technology Development Group, U. R. Rao Satellite Centre  
Bangalore, India-560017

(received October 3, 2020; accepted March 5, 2021)

Cylindrical shells made of composite material form one of the major structural parts in aerospace structures. Many of them are acoustically thick, in which the ring frequencies are much higher than their critical frequencies. In this work, sound radiation behaviour of acoustically thick composite cylinders is presented. Based on the structural and acoustic wave number diagrams, the modal average radiation resistances in the frequency band of interest are theoretically determined. The structural wavenumbers are determined considering transverse shear deformation. The results show lesser sound radiation between the critical and ring frequencies, and significant sound radiation near the ring frequency and beyond. In the absence of the present results the radiation efficiency is considered to be unity at all frequencies beyond the critical frequency, including near the ring frequency. The radiation resistances of the same cylinder are determined experimentally and they are in very good agreement with the theoretical estimates. As part of this investigation, an expression for determining the ring frequency of composite cylinder is also presented.

**Keywords:** radiation resistance; radiation efficiency; cylindrical shells; composites; ring frequency; critical frequency; SEA



Copyright © 2021 S. Josephine Kelvina Florence, K. Renji  
This is an open-access article distributed under the terms of the Creative Commons Attribution-ShareAlike 4.0 International (CC BY-SA 4.0 <https://creativecommons.org/licenses/by-sa/4.0/>) which permits use, distribution, and reproduction in any medium, provided that the article is properly cited, the use is non-commercial, and no modifications or adaptations are made.

## Nomenclature

Symbols not listed here are used only at specific places and are explained wherever they occur.

$p_i$  – acoustic pressure in subsystem  $i$ ,  
 $A$  – area of the cylindrical shell,  
 $D_{ij}$  – bending stiffness terms,  
 $f_c$  – critical frequency in Hz,  
 $m_e$  – coefficient that depends on temperature and humidity,  
 $\frac{m\pi}{L}$  – function of axial half wavenumber,  
 $\frac{n}{a}$  – function of circumferential full wavenumber,  
 $c_l$  – longitudinal wave speed,  
 $L$  – length of the cylindrical shell,  
 $\rho_m$  – mass per unit area,  
 $\rho$  – material density,  
 $d$  – mean free path of the chamber,  
 $n_2$  – modal density of the cylinder,  
 $n_1$  – modal density of the reverberation chamber,  
 $f_{mn}$  – natural frequency in Hz,

$N(\omega)$  – number of modes below the radian frequency  $\omega$ ,  
 $n(f)$  – number of modes per Hz,  
 $\sigma_{\text{rad}}$  – radiation efficiency,  
 $R_{\text{rad}}$  – radiation resistance,  
 $a$  – radius of the cylindrical shell,  
 $T_{60}$  – reverberation time in seconds,  
 $f_r$  – ring frequency in Hz,  
 $\omega_r$  – ring frequency in rad/s,  
 $N$  – shear rigidity of the shell,  
 $\alpha_w$  – sound power absorption coefficient of the walls,  
SPL – sound pressure level,  
 $\langle a \rangle_x$  – spatial average acceleration response ,  
 $\langle v \rangle_x$  – spatial average velocity response,  
 $\rho_o c_o$  – specific acoustic impedance,  
 $S$  – surface area of the reverberation chamber,  
 $\bar{\alpha}$  – total sound power absorption coefficient,  
 $V$  – volume of the reverberation chamber,  
 $k_y$  – axial wave number,  
 $k$  – wave number.

## 1. Introduction

Composite shells are extensively used in aerospace structures as they possess low mass with high strength and stiffness and hence information on their sound radiation characteristics is important. One of the critical loading conditions for aerospace structures is the acoustic excitation. The fluctuating pressures associated with the acoustic energy cause severe dynamic loading which are broadband in nature ranging from 20–8000 Hz. Responses induced as a result of acoustic loads are directly related to acoustic radiation resistances of the structure. In both contexts, information on the sound radiation characteristics of composite cylindrical shells is desired. Sound radiation characteristics of a cylinder are dependent on two important parameters, viz., the ring frequency and the critical frequency. Cylinders are termed as acoustically thin when the ring frequency is less than that of the critical frequency and acoustically thick when the ring frequency is higher than that of critical frequency.

One of the earliest works on the sound radiation of cylinder is by BORDONI and GROSS (1948) and a detailed analytical treatment is presented by RUNKLE and HART (1969). If the modal densities of the structure under consideration are quite high, deterministic approaches are very cumbersome in computing the radiation resistance. They are suitable only when the radiation resistance at a particular mode is desired. When the modal overlap is high, statistical approaches are commonly used in defining the radiation characteristics. Statistical Energy Analysis (SEA) is a framework by which the responses of higher order modes are generally determined. Here the radiation resistances are obtained based on the physical argument of the nature of modes, whether it is acoustically fast or slow, and the number of modes present in the frequency band (MANNING, MAIDANIK, 1964). In an acoustically fast mode, the structural wavenumber is lesser than the acoustic wave number and vice versa. The sound radiated by acoustically fast mode is significantly high compared to the sound radiated by an acoustically slow mode.

Sound radiation characteristics of isotropic cylindrical shells was extensively investigated by MANNING and MAIDANIK (1964). They presented a classic explanation for the radiation characteristics of cylindrical shells. Radiation efficiency shows two distinct peaks one at the ring frequency and the other at the critical frequency. SZECHENYI (1971) obtained the radiation characteristics of isotropic cylinder for various ratios of ring and critical frequency by considering the number of acoustically fast modes present in the frequency band of interest. Addressing both acoustically fast and acoustically slow modes, researchers proposed formulae for radiation ratios of acoustically thin isotropic cylinder (MILLER, FAULKNER, 1983). In all the above

works, the radiation properties are determined for modal distribution of surface velocities. To determine the radiated sound power for a given velocity distribution, expressions in the form of integrals are presented (STEPANISHEN, 1978). There are several other works on the sound radiation from isotropic cylinders (BURROUGHS, 1984; LAULAGNET, GUYADER, 1989; RAMACHANDRAN, NARAYANAN, 2007; SUN *et al.*, 2018). All these studies are applicable for lower order modes of acoustically thin cylinders. Few works reported pertains to the sound field in a cavity formed by the cylinder, again in the lower order modes (FAHY, 1969; 1970; QIAO *et al.*, 2013). It is important to note that the cylinders considered in all the above works are acoustically thin and made of isotropic material.

On the other hand, the works that are reported on the radiation characteristics of composite cylinders are very few. YIN *et al.* (2009) presented numerical results for the far-field acoustic pressure of fluid loaded composite laminated shells stiffened with rings. Authors studied the effect of ply-angles and damping factors on the far-field acoustic radiation characteristics and concluded that the lamination scheme has little effect on the acoustic radiation. Other works related to sound radiation from composite cylinders deal with acoustically thin cylinders (CAO *et al.*, 2012; ZHAO *et al.*, 2015).

It is seen that most of the works reported are on acoustically thin cylinders and the results for acoustically thick cylinders are rarely reported. Few researchers studied the radiation characteristics of an acoustically thick cylinder. WANG and LAI (2000) presented an approximate method to compute modal averaged radiation resistance of finite length isotropic cylindrical shells. They compared the modal radiation efficiency computed using approximate expression with that obtained using boundary element method. It was concluded that for acoustically thick shells, both subsonic and supersonic modes exist below the critical frequency. They considered the radiation efficiency of the acoustically thick cylinder to be unity at frequencies above its critical frequency, even near the ring frequency. Also, they considered isotropic cylindrical shells in their work.

Several cylinders used in spacecraft structure are made of composite material and they are acoustically thick. It is seen that though there are several works reported on the radiation characteristics of cylindrical shells, the cylinders considered are made of isotropic materials. Works related to composite cylinders are seldom reported. Also, the studies carried out are on acoustically thin cylinders and works on acoustically thick cylinders are not frequently reported. In the case of acoustically thick isotropic cylinder, the radiation efficiency beyond the critical frequency is taken as unity (SZECHENYI, 1971; WANG, LAI, 2000). Also, all these works do not consider transverse shear deformation

while determining the wave numbers, which is influential in the higher order modes. Further, the studies reported on acoustically thick cylinders are based on numerical simulation and no experimental results are presented which can be used to verify the radiation efficiencies at frequencies above the critical frequencies.

In this work, sound radiation characteristics of a typical acoustically thick composite cylinder are obtained theoretically. They are determined based on the nature of the modes, as done for structures having high modal overlap. Transverse shear deformation is also considered while determining the wave numbers. It is seen that the radiation efficiencies of acoustically thick cylinders need not be unity at frequencies above critical frequencies and they can be much higher. These results are then verified through experiments. An expression for determining the ring frequencies of composite cylinders is also derived.

## 2. Details of the cylinder

An acoustically thick composite cylinder is considered for the investigations. Since the experiments are carried out on a particular cylinder, the theoretical estimation is also carried out for the same cylinder. The cylinder is of honeycomb sandwich construction with face-sheets made up of composite material. The structural properties of the cylinder are presented below. In earlier works, the modal density (JOSEPHINE *et al.*, 2018) and critical frequency of the same cylinder were obtained experimentally (RENJI, JOSEPHINE, 2020).

### 2.1. Geometric and elastic properties of the cylinder

The properties of the cylinder are as follows

length	1.485 m,
radius	0.597 m,
area	5.578 m <sup>2</sup> ,
mass per unit area	1.72 kg/m <sup>2</sup> ,
face sheet thickness	0.290 mm,
face sheet material	4 layers of CFRP: (0/90)/35°/0°/-35°,
core material	aluminium honey comb,
core height	12 mm,
core density	32 kg/m <sup>3</sup> ,
core shear modulus	1.4 · 10 <sup>8</sup> N/m <sup>2</sup> ,
shear rigidity <i>n</i>	17.6 · 10 <sup>5</sup> N/m,
$A_{11}$	$= 8.22 \times 10^7$ N/m,
$A_{22}$	$= 3.30 \times 10^7$ N/m,
$A_{12}$	$= 1.39 \times 10^7$ N/m,
$A_{66}$	$= 1.48 \times 10^7$ N · m,
$D_{11}$	$= 3.11 \times 10^3$ N · m,
$D_{22}$	$= 1.27 \times 10^3$ N · m,
$D_{12}$	$= 52.2$ N · m,
$D_{66}$	$= 55.5$ N · m.

Suffix 1 represents the longitudinal direction and suffix 2 refers to the tangential direction.

### 2.2. Ring frequency of the cylinder

Ring frequency is the frequency at which the cylinder undergoes uniform expansion and contraction; in other words, the cylinder does not undergo bending deformation. It is the frequency at which the wave length of the in plane wave equals the circumference of the cylinder. If  $c_l$  is the speed of the in plane wave, the ring frequency of a cylinder having radius  $a$  is  $\omega_r = c_l/a$ . The speed of the in plane wave in a cylinder made of isotropic material having Young's modulus  $E$ , Poisson's ratio  $\mu$  and density  $\rho$  is  $c_l^2 = \frac{E}{\rho(1-\mu^2)}$ . Hence, the ring frequency of the cylinder is given by

$$\omega_r^2 = \frac{E}{\rho(1-\mu^2)a^2}. \tag{1}$$

There is no expression reported for estimating the ring frequency of a composite cylinder. In the absence of any expression for estimating the ring frequency of a composite shell, an approximation could be to use the expression for isotropic shells with the properties replaced by the properties of the composite shell. Denoting  $A_{ij}$  as the extensional stiffness term in the standard ABD matrix of composite plates, the ring frequency can be determined approximately using the relation

$$\omega_r^2 = \frac{A_{22}}{\rho_m a^2}. \tag{2}$$

Here, suffix 1 stands for the longitudinal direction of the cylinder and suffix 2 stands for the tangential (circumferential) direction. At the ring frequency, only tangential strains are generated and therefore it is logical to use the extensional stiffness  $A_{22}$  for determining the ring frequency.

Further, the cylinder undergoes uniform radial motion at the ring frequency. This implies that the derivatives of the displacement along two in-plane directions vanish (GHINET *et al.*, 2006). Authors used this property and derived the expression for the ring frequency as

$$\omega_r^2 = \frac{A_{22} - \frac{B_{22}}{a}}{\rho_m a^2}. \tag{3}$$

For a symmetric laminate  $B_{ij} = 0$  and hence the expression for the ring frequency becomes the same as given by Eq. (2). Therefore, the existing literature suggests the expression for ring frequency as given by Eq. (2).

A close examination of Eq. (2), which is for an isotropic material, reveals that the ring frequency depends on Young's modulus and Poisson's ratio. It is to be noted that the isotropic material has two independent elastic constants and the ring frequency depends on both. In a similar fashion it is expected that the ring frequency of a composite shell shall depend on all the four elastic constants. But the expression for ring frequency for composite shells given by Eq. (2)

shows that the ring frequency depends on  $A_{22}$ , which means that the ring frequency depends on two elastic properties, namely  $E_{tt}$  and  $\mu_{lt}$  where  $l$  stands for fibre direction and  $t$  stands for transverse direction in a lamina. Hence, obtaining ring frequencies through other considerations is investigated.

Characteristic of in plane waves in composite plates was investigated by Renji and he suggested an expression to determine the speed of the in plane waves (RENJI *et al.*, 2020). It was shown that there exist two in-plane waves in a composite plate, one dominated in longitudinal motion and the other dominated in in-plane shear motion. The speed of the longitudinal motion dominant in plane wave is

$$c_l^2 = \frac{A_{22}}{\rho_m} \left[ 1 + 0.25\beta - \left\{ \frac{1 - \alpha^2 - 2\alpha\beta}{8} \right\} \right]. \quad (4)$$

Accordingly, the ring frequency of the composite cylinder is given by

$$\omega_r^2 = \frac{A_{22}}{\rho_m a^2} \left[ 1 + 0.25\beta - \left\{ \frac{1 - \alpha^2 - 2\alpha\beta}{8} \right\} \right], \quad (5)$$

where  $\alpha = \frac{A_{12}}{A_{22}}$ ,  $\beta = \frac{A_{66}}{A_{22}}$ . The factor over the existing approximate expression is  $\left[ 1 + 0.25\beta - \left\{ \frac{1 - \alpha^2 - 2\alpha\beta}{8} \right\} \right]$  and it depends on the values of the parameters  $\alpha$  and  $\beta$ . In this specific case the influence is small.

The ring frequency depends on the elastic properties  $A_{11}$ ,  $\alpha$  and  $\beta$  and it assumes  $A_{11} = A_{22}$ . Thus, it can be seen that the ring frequency depends on all the elastic properties. Even for the isotropic material, the ring frequency depends on these properties but these properties are related to each other.

In a practical situation  $A_{11} \neq A_{22}$ . Therefore, one way of using the above expression is to consider the elastic property along the tangential direction. This is justifiable as the cylinder undergoes tangential strains at the ring frequency and the longitudinal strains are negligible. It is possible that in cases where  $A_{11} \neq A_{22}$ , another frequency of interest can be present which is characterized by  $A_{11}$  but this frequency may not have influence as significant as the ring frequency characterized by  $A_{22}$ .

The ring frequency of this cylinder is estimated as 1200 Hz.

### 2.3. Critical frequency of the cylinder

Yet another parameter of interest in sound radiation is the critical frequency of the cylinder which is related to the speed of flexural waves. It is well known that the curvature increases the flexural wave speed in cylinders and as a result it matches the acoustic wave speed at an earlier frequency as compared to that flat of plates. An expression for critical frequency of composite cylinders derived earlier (RENJI, JOSEPHINE, 2020) is given below

$$\omega_c^2 = \omega_{c,p}^2 \left[ 1 - \left( \frac{\omega_r}{\omega_c} \right)^2 \left( \frac{k_y}{k} \right)^4 \right], \quad (6)$$

where  $\omega_c$  is the critical frequency of the cylinder and  $\omega_{c,p}$  is the critical frequency if it were a plate. Using the above expression, the critical frequency of the cylinder is computed as 495 Hz.

It should be noted that the ring frequency of this cylinder is greater than that of the critical frequency and the cylinder belongs to acoustically thick category.

### 2.4. Modal density of the cylinder

The modal densities of the cylinder are theoretically obtained using the expression (JOSEPHINE *et al.*, 2018) and the results in one-third octave bands are presented in Table 1. It is to be noted that the theoretical expression incorporates transverse shear effects and it gives modal densities very close to the experimentally obtained values (RENJI, JOSEPHINE, 2020).

Table 1. Modal density of the cylinder.

Sl. No.	Frequency [Hz]	Modal density [Hz <sup>-1</sup> ]
1	400	0.056
2	500	0.066
3	630	0.077
4	800	0.096
5	1000	0.124
6	1250	0.148
7	1600	0.127
8	2000	0.132
9	2500	0.142
10	3150	0.156
11	4000	0.181
12	5000	0.211
13	6300	0.250
14	8000	0.300

## 3. Theoretical estimation of radiation resistance

Acoustic radiation characteristics of a structure can be described by the parameter radiation resistance. Radiation resistance of a structure, denoted by  $R_{\text{rad}}$ , is a measure of the sound power radiated by the structure  $W$ . They are related by

$$W = R_{\text{rad}} \langle v^2 \rangle_x, \quad (7)$$

where  $\langle v^2 \rangle_x$  is the spatial average value of the velocity of the structure. Another related parameter is the radiation efficiency denoted by  $\sigma_{\text{rad}}$ , which is the ratio of the sound power radiated by the structure to the sound power radiated by a piston having the same area and mean square value of velocity. The radiation efficiency is related to radiation resistance by

$\sigma_{rad} = R_{rad}/(\rho_o c_o A)$  where  $A$  is the radiating area and  $\rho_o c_o$  is the characteristic impedance of the acoustic medium. The objective is to determine the modal average radiation characteristics in the frequency band of interest.

Vibration modes can be classified into acoustically fast or supersonic modes and acoustically slow or subsonic modes. This classification depends on the magnitude of the structural wave number in comparison with acoustic wave numbers. Acoustically fast modes are characterised by lower structural wavenumber compared to the acoustic wave number and they radiate sound well. The acoustically slow modes radiate very less. Modal averaged radiation resistance can be ascertained by knowing the number of acoustically fast modes and the total number of vibration modes in a particular band of interest.

The number of acoustically fast modes in the given frequency band can be determined from their wavenumber diagrams. Closed form expression available for determining the modal density of composite cylinders (JOSEPHINE *et al.*, 2018) is used to compute the total number of modes in the given band. Radiation ratio, denoted by  $\sigma_{rad}$ , is then obtained as the ratio of the number of acoustically fast modes to the total number of modes in that frequency band times the radiation efficiency of the acoustically fast mode.

### 3.1. Mode count of acoustically fast modes

The number of acoustically fast modes in the given band is obtained from the structural and acoustic wave number diagrams. The expression for the natural frequency of a composite cylinder is given by (JOSEPHINE *et al.*, 2018)

$$f_{mn}^2 = \frac{1}{4\pi^2 \rho_m \left[ 1 + \left( \frac{D_{11}}{N} \bar{m}^2 + \frac{D_{22}}{N} \bar{n}^2 \right) \right]} \cdot \left\{ D_{11} \bar{m}^4 + 2(D_{12} + 2D_{66}) \bar{m}^2 \bar{n}^2 + D_{22} \bar{n}^4 + \frac{A_{11} A_{22} - A_{12}^2}{a^2} \bar{m}^4 \left[ 1 + \frac{D_{11}}{N} \bar{m}^2 + \frac{D_{22}}{N} \bar{n}^2 \right] \right\} \frac{1}{A_{11} \bar{m}^4 + A_{22} \bar{n}^4 + \frac{A_{11} A_{22} - A_{12}^2 - 2A_{12} A_{66}}{A_{66}} \bar{m}^2 \bar{n}^2}, \quad (8)$$

where  $\rho_m$  is the mass per unit area of the cylinder,  $N$  is the shear rigidity,  $A_{ij}$  is the extensional stiffness, and  $D_{ij}$  is the bending stiffness of the section of the cylinder. The cylinder has a length of  $L$  and radius of  $a$ . The above expression considers transverse shear deformation which influences the frequencies of higher order modes.

At a particular frequency, the bending wave in the cylinder has both axial wave number and circumferential wave number. These are represented by the terms  $\bar{m} = \frac{m\pi}{L}$  and  $\bar{n} = \frac{n}{a}$  in the expression for natural frequency.

Equation (8) represents the relationship between the wavenumbers in a composite cylinder at a particular frequency. The above relation takes into account the transverse shear deformation. At a particular one-third octave band centre frequency, values of  $\bar{m}$  can be calculated for various values of  $\bar{n}$ . Loci of these values represent the structural wave number diagram at that frequency. This procedure is repeated for the upper and lower limit of the particular frequency band. Figure 1 shows the structural wavenumber diagrams for 315 Hz, 400 Hz, 500 Hz and 630 Hz 1/3 octave bands. In case of thin plates, the structural wavenumber diagram is a quarter of a circle. Due to curvature the points shift towards circumferential wave number axis.

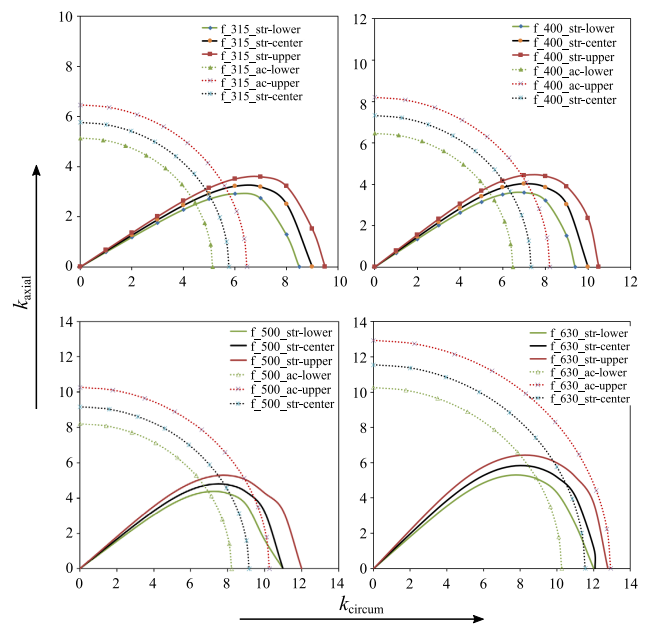


Fig. 1. Structural and acoustic wavenumber diagrams.

Acoustic wavenumber diagrams are drawn using the relation between frequency, wavenumber and speed of sound in air which is 343 m/s. Acoustic wave number diagrams are quarter circle at any frequency. They are also shown in Fig. 1. Continuous line represents the structural wave number diagram and the dotted line represents the acoustic wave number diagram.

Area of closed loop polygon where the structural wave numbers are less than that of the acoustic wave number represents the number of acoustically fast modes in a particular frequency band. Thus, the area given by the closed loop polygon ACBA represents the number of acoustically fast modes. The structural wave number and the acoustic wave number diagrams always intersect at frequencies up to 500 Hz 1/3 octave band. In 630 Hz band, the structural wave number and the acoustic wave number diagrams do not intersect at its upper limit. This implies that above this frequency band, all the modes are acoustically fast.

### 3.2. Total mode count

Total number of modes  $N(\omega)$  in the frequency band of interest  $\Delta\omega$  can be found using the expression (JOSEPHINE *et al.*, 2018)

$$N(\omega) = \frac{aL}{\pi} \int_0^{\pi/2} \left[ \frac{\rho_m \omega^2 - f_3}{2f_1} \left\{ \frac{f_2}{N} + \sqrt{\left( \frac{f_2}{N} \right)^2 + \frac{4f_1}{\rho_m \omega^2 - f_3}} \right\} \right] d\theta, \quad (9)$$

where

$$f_1 = D_{11}c^4 + 2(D_{12} + 2D_{66})c^2s^2 + D_{22}s^4,$$

$$f_2 = D_{11}c^2 + D_{22}s^2,$$

$$f_3 = \frac{(A_{11}A_{22} - A_{12}^2)c^4}{A_{11}c^4 + A_{22}s^4 + \frac{A_{11}A_{22} - A_{12}^2 - 2A_{12}A_{66}}{A_{66}}c^2s^2},$$

and  $f_1$ ,  $f_2$  and  $f_3$  are the functions representing the orthotropic parameters. Structural mode count in a particular frequency band is evaluated numerically integrating Eq. (9). The expression for the mode count considers transverse shear deformation which influences the mode count of the higher order modes.

### 3.3. Radiation efficiency

Radiation efficiency or radiation ratio denoted by  $\sigma_{\text{rad}}$  is calculated based on the total number of acoustically fast modes relative to the total number of modes in the frequency band under consideration. This can be mathematically written as

$$\sigma_{\text{rad}} = \left[ \frac{\text{total no. of acoustically fast modes}}{\text{total no. of modes}} \right] \cdot \sigma_{\text{fast}}. \quad (10)$$

Equation (10) is used to determine the radiation efficiency of the structure in the frequency band of interest. The term inside the braces of Eq. (10) is determined from the wave number diagrams and it is always less than unity. If all the modes are acoustically fast, this term is unity. The second term of the above equation  $\sigma_{\text{fast}}$  represents the radiation efficiency of acoustically fast modes. Radiation efficiency of these acoustically fast modes can be considered as unity. Above the critical frequency some of the modes will be acoustically slow and some of the modes will be acoustically fast. Therefore, effectively the radiation efficiency will be less than unity. If all the modes are acoustically fast, the radiation efficiency will be unity.

Beyond the ring frequency, curvature effects are negligible and therefore radiation efficiency can be computed using the expression for plates

$$\sigma_{\text{rad}} = \left\{ 1 - \frac{f_c}{f} \right\}^{-(1/2)} \quad \text{for } f > f_r. \quad (11)$$

Based on the above arguments and using Eq. (10), the radiation efficiencies of the cylinder are computed. They are presented in Table 2. Radiation resistance is determined from the radiation efficiency.

Table 2. Estimated radiation efficiency and radiation resistance of the cylinder.

Sl. No.	Frequency [Hz]	$\sigma_{\text{rad}}$	$R_{\text{rad}}$ [W/(m/s) <sup>2</sup> ]
1	315	0.165	381.46
2	400	0.228	527.10
3	500	0.300	693.56
4	630	1.000	2311.85
5	800	1.000	2311.85
6	1000	1.580	3655.36
7	1250	1.390	3205.96
8	1600	1.260	2924.29
9	2000	1.200	2763.19
10	2500	1.150	2651.88
11	3150	1.110	2569.48
12	4000	1.080	2507.56
13	5000	1.070	2464.44
14	6300	1.050	2430.49
15	8000	1.040	2403.75
16	10000	1.030	2384.49

The results show a peak in the radiation efficiency near the ring frequency. The results reported earlier on the radiation characteristics of acoustically thick cylinders (SZECHENYI, 1971; WANG, LAI, 2000) do not present any peak near the ring frequency. That is because in those studies at frequencies above the critical frequency, the radiation efficiency is considered to be unity. It needs to be noted that the wavenumbers in the present work are calculated considering transverse shear deformation along with the orthotropic nature of composite cylinder, which were not considered in earlier works.

While deriving these characteristics it is assumed that the cylinder is infinitely long, meaning that the boundary conditions at the end of the cylinder do not affect the characteristics. Works reported on finite length cylindrical shells reveals that the modal radiation efficiencies of finite length cylindrical shells approach to those of infinite cylindrical shells at higher frequencies (WANG, LAI, 2001; FYFE, ISMAIL, 1989; LIN *et al.*, 2011). These results justify the assumption of the cylinder being infinitely long while determining the radiation characteristics in the higher order modes.

## 4. Experimental radiation resistance

As the theoretical estimates show significant sound radiation at frequencies above critical frequencies, it is thought that it would be good to see how the experi-

mental radiation efficiencies are. The radiation efficiencies of the same cylinder are obtained experimentally and these results are presented here.

#### 4.1. Experimental methodology

The cylinder is suspended freely in a reverberation chamber. It is excited using an electro-dynamic shaker. The radiation resistance of the cylindrical shell can be determined from the measured vibration response of the structure and the Sound Pressure Level (SPL) in the reverberation chamber. The methodology is developed by applying SEA to the cylinder-reverberation chamber system. Few researchers used reciprocity technique to measure the radiation efficiency where the responses are measured for a known acoustic excitation and the radiation resistance is obtained (SQUICCIARINI *et al.*, 2015). This is an indirect method of deriving the radiation resistance and it involves several uncertainties. Therefore, the direct method where the structure is excited using shaker is used in the present work.

In the SEA model the acoustic field is taken as subsystem 1 and the structure is taken as subsystem 2. Both the acoustic and the vibration fields are assumed to be diffused. Considering the power balance of subsystem 1,

$$\pi_1 = \omega (\eta_1 + \eta_{12}) E_1 - \omega \eta_{21} E_2. \quad (12)$$

Here  $\pi_1$  is input power in subsystem 1;  $\eta_i$  is dissipation loss factor of the respective subsystem;  $\eta_{ij}$  is coupling loss factor when the power flow is from subsystem  $i$  to  $j$  and  $E_i$  is energy of the respective subsystem.

Since the power input to subsystem 1 is zero, the energies of the two subsystems are related by

$$E_1 = \frac{\eta_{21}}{\eta_1 + \eta_{12}} E_2. \quad (13)$$

The energy of the acoustic field  $E_1$  in terms of the pressure  $p$  is (REYNOLDS, 1981)

$$E_1 = \frac{\langle p^2 \rangle_x}{\rho_o c_o^2} V, \quad (14)$$

where  $V$  is the volume of the chamber. The energy of the structure  $E_2$  can be obtained from the measured velocity as

$$E_2 = \rho_m A \langle v^2 \rangle_x. \quad (15)$$

The coupling loss factor denoted by  $\eta_{21}$  is related to  $R_{\text{rad}}$  as (NORTON, 1989)

$$\eta_{21} = R_{\text{rad}} / (\rho_m \omega A). \quad (16)$$

Combining Eqs (13)–(16) we get

$$R_{\text{rad}} = \omega \{ \eta_1 + \eta_{12} \} \frac{V}{\rho_o c_o^2} \frac{\langle p^2 \rangle_x}{\langle v^2 \rangle_x}. \quad (17)$$

The coupling loss factor  $\eta_{12}$  is computed from the reciprocal relationship (LYON, 1975)

$$\eta_{12} = \eta_{21} (n_2 / n_1), \quad (18)$$

and then the expression for the radiation resistance becomes

$$R_{\text{rad}} = \frac{\omega V}{\rho_o c_o^2} \eta_1 \frac{\langle p^2 \rangle_x}{\langle v^2 \rangle_x} \left\{ 1 - \frac{\omega V}{\rho_o c_o^2} \frac{n_2}{n_1} \frac{1}{\rho_m \omega A} \frac{\langle p^2 \rangle_x}{\langle v^2 \rangle_x} \right\}^{-1}. \quad (19)$$

The dissipation loss factor of the acoustic field is a measure of the sound absorbed by the reverberation chamber. The dissipation loss factor of the chamber having surface area  $S$  and sound absorption coefficient of  $\bar{\alpha}$  is (LYON, 1975)

$$\eta_1 = \frac{S c \bar{\alpha}}{8 \pi f V}. \quad (20)$$

The radiation resistance of the structure is now given by

$$R_{\text{rad}} = \frac{\langle p^2 \rangle_x S \bar{\alpha}}{4 \rho_o c_o \langle v^2 \rangle_x - \{ n_2 c^2 / \pi f^2 \rho_m A \} \langle p^2 \rangle_x}. \quad (21)$$

Knowing the sound absorption by the reverberation chamber, the radiation resistance of the structure can be determined using Eq. (22) by measuring the acoustic field in the room and the corresponding vibration field of the structure.

#### 4.2. Sound power absorption coefficient of the chamber

The sound absorption coefficient of  $\bar{\alpha}$  of a room is related to the sound absorption coefficient of the walls and that of the air  $\alpha_w$  through the relation (REYNOLDS, 1981)

$$\bar{\alpha} = \frac{\alpha_w + m_e d - (m_e^2 d^2 / 2)}{1 - [\alpha_w + m_e d - (m_e^2 d^2 / 2)]}, \quad (22)$$

where  $d$  is the mean free path of the acoustic cavity given by  $4V/S$  and  $m_e$  is a energy attenuation coefficient that varies with temperature and humidity of the medium. The parameter  $m_e$  is computed using the formula (COX, D'ANTONIO, 2004) for this range of humidity (20–70%)

$$m_e = 5.5 \cdot 10^{-4} \cdot \frac{50}{h} \cdot \left( \frac{f}{1000} \right)^{1.7}. \quad (23)$$

Here  $h$  represents the humidity and  $f$  is the frequency in Hz. The total sound absorption coefficient denoted by  $\bar{\alpha}$  can be determined from the known values of the properties of the medium and the sound absorption

coefficient of the walls. The sound power absorption coefficient of the walls can be determined from the measured reverberation time using the relation (RENJI *et al.*, 1998)

$$T_{60} = 55.26 \frac{V/cS}{\ln(1 - \alpha_w)^{-1} + md}. \quad (24)$$

Reverberation time is the time taken to decay the SPL by 60 dB after the sound source is switched-off and this parameter is experimentally determined. The chamber is excited through a loud speaker. The sound field inside the chamber is measured using microphones and the data is recorded. The excitation is abruptly stopped and the sound field now decays. The time taken for the sound level to fall by 60 dB after the excitation is stopped and determined. This is specified in 1/3-rd octave bands over the selected frequency range. The measured reverberation time of the chamber is given in Fig. 2.

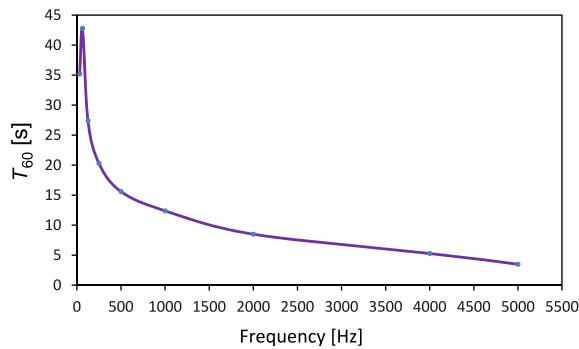


Fig. 2. Reverberation time of the chamber.

The experiment is conducted in air with a relative humidity of 50% and temperature of 22°C. The values of  $m_e d$  corresponding to the above conditions of the medium are shown in Fig. 3. The dimensions of the chamber are  $9.0 \times 11.3 \times 14.3$  m, having a volume of  $1454 \text{ m}^3$  and surface area of  $784 \text{ m}^2$ . The sound power absorption coefficients of the walls are presented in Fig. 4. The sound power absorption coefficients of the chamber (which includes the effect of absorption due to walls and air) computed using Eq. (22) are shown in Fig. 5.

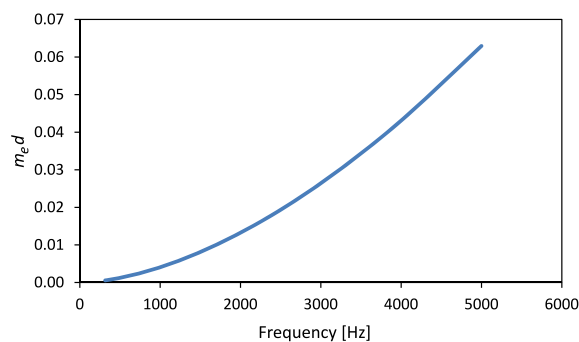


Fig. 3. Values of the parameter  $m_e d$ .

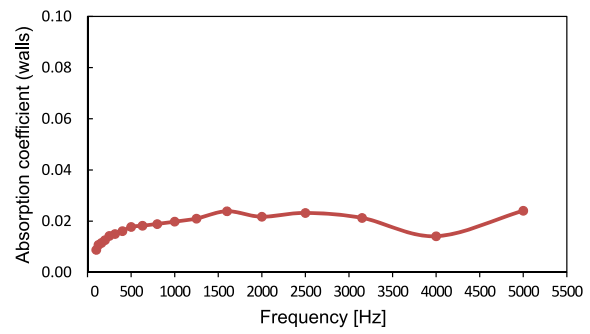


Fig. 4. Sound power absorption coefficients of the walls.

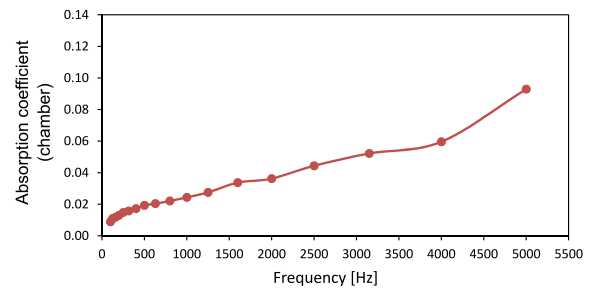


Fig. 5. Sound power absorption coefficient of the chamber.

#### 4.3. Details of radiation resistance test

The cylinder is hung in the reverberation chamber, shown in Fig. 6. The cylinder is excited at two locations (shown in Fig. 7) using electro-dynamic shaker system, one location at a time. When excited at one



Fig. 6. The cylinder being excited by a shaker.

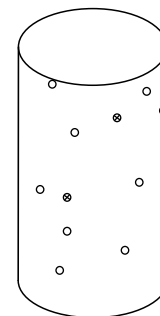


Fig. 7. Drive point locations  $\otimes$  and accelerometer locations  $\circ$ .

location the accelerations are measured at 9 locations and the sound field is measured at 3 locations far away from the cylinder as well as the walls. The locations of accelerometers and microphones are given in Tables 3 and 4, respectively. It should be noted that minimum circumferential distance between accelerometer is 0.30 m and no two accelerometers are positioned in the same height as is evident from the following table. For the microphone locations the coordinates are given with the centre of the floor of the chamber as origin.

Table 3. Accelerometer locations in cylinder.

Accelerometer No.	Location	
	Circumference [°]	Axial distance [mm]
A1	30	200
A2	90	400
A3	150	600
A4	210	800
A5	270	1000
A6	310	1200
A7	250	700
A8	120	500
A9	180	300

Table 4. Microphone locations.

Microphone No.	Location	
	Coordinate [m]	Height above ground [m]
M1	(-2.5, -1)	2.5
M2	(1.6, -1)	1.5
M3	(-2, 1)	1.82

The spatial average of the acceleration and SPL give the vibration and the corresponding acoustic field and the results are given in Table 5. The spatial average of the acceleration is the spatial average of the mean square value of acceleration. Similarly, spatial average SPL is from the spatial average of means square value of pressure. The experiment is performed for two driving points.

The sound field is measured using 1/2" condenser type microphone. The sensitivity of the microphone is about 12.7 mV/Pa. As it is of 1/2" size, correction factors are to be applied when a random incidence field is measured. At 3000 Hz it is 0.5 dB, at 4000 Hz it is 1.0 dB and at 5000 Hz it is 1.5 dB. To arrive at the correct SPL, these values are added to the measured values.

#### 4.4. Measured radiation resistance

Based on the results given in Table 5, the radiation resistance of the cylinder is determined using Eq. (21). The results are presented in Table 6.

The sound field and the vibration field are considered to be diffused. To ensure diffuse vibrational field, the structure under consideration should possess large number of modes in the frequency band of interest (LE BOT, COTONI, 2010). In the 1/3 octave band centred at 500 Hz, the cylinder under consideration has 7.6 modes and it is still higher at higher frequencies. Similarly, the modes available in the acoustic field are quite high. 500 Hz 1/3 octave band has more than 12000 modes as the volume of the chamber is quite high. Thus, we see that the acoustic and vibration fields can be very well assumed to be diffusive. The measured results also show that no significant variation of responses (both acceleration and SPL) with location is seen.

Table 5. Spatial average of measured SPL and accelerations for various drive points.

Sl. No.	Frequency [Hz]	Location 1		Location 2	
		SPL [dB]	$\langle a \rangle_x$ [g]	SPL [dB]	$\langle a \rangle_x$ [g]
1	315	78.12	0.27	81.34	0.39
2	400	85.88	0.39	83.83	0.46
3	500	90.34	0.56	84.50	0.39
4	630	87.51	0.50	86.67	0.43
5	800	87.00	0.52	87.67	0.51
6	1000	83.67	0.38	84.00	0.40
7	1250	85.13	0.70	85.07	0.83
8	1600	86.00	0.95	85.57	1.03
9	2000	85.40	1.26	85.20	1.48
10	2500	76.83	0.60	78.13	0.94
11	3150	69.33	0.45	70.67	0.67
12	4000	65.17	0.45	67.50	0.70
13	5000	65.33	0.67	68.83	1.32

Table 6. Measured radiation resistance and radiation efficiency of the cylinder.

Sl. No.	Frequency [Hz]	$R_{\text{rad}}$ [W/(m/s) <sup>2</sup> ]	$\sigma_{\text{rad}}$
1	315	107.56	0.047
2	400	440.79	0.191
3	500	1132.98	0.490
4	630	1625.87	0.703
5	800	2465.40	1.060
6	1000	3158.16	1.360
7	1250	1983.80	0.858
8	1600	2683.76	1.160
9	2000	2132.00	0.922
10	2500	2336.59	1.010

Compared to radiation resistance, the radiation efficiency can give clearer understanding on the radiation characteristics. Therefore, the radiation efficiencies are determined subsequently and the results are given in Table 6 and Fig. 8.

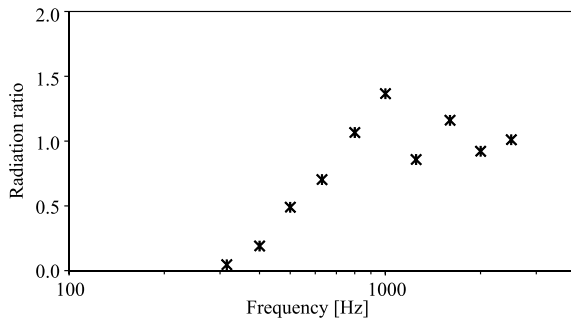


Fig. 8. Measured radiation efficiency of the cylinder.

To attach the stringer of the shaker to the cylinder, a small threaded metal piece (15 × 15 mm) is bonded on the outer face sheet. At high frequencies this type of excitation can cause the outer face sheet alone to vibrate significantly resulting in different vibration modes. Hence, the measured accelerations will not correspond to the panel bending mode but it will include the face sheet bending modes and therefore the radiation resistance deduced will not be correct. Therefore, the results are given only up to 2500 Hz band in Table 6 and Fig. 8. At frequencies beyond 2500 Hz band the radiation efficiency can be taken as unity based on the fact that well above the ring frequency the radiation efficiency of a cylinder approaches that of a plate and the radiation efficiency of a plate is unity at frequencies well above its critical frequency.

## 5. Results and discussion

Radiation efficiency obtained through experimental investigations are compared with the analytically determined results in Table 7 and Fig. 9.

Table 7. Estimated and measured radiation efficiency of the cylinder.

Sl. No.	Frequency [Hz]	$\sigma_{\text{rad}}$	
		Theory	Experiment
1	315	0.165	0.047
2	400	0.228	0.191
3	500	0.300	0.490
4	630	1.000	0.703
5	800	1.000	1.060
6	1000	1.580	1.360
7	1250	1.390	0.858
8	1600	1.260	1.160
9	2000	1.200	0.922
10	2500	1.150	1.010

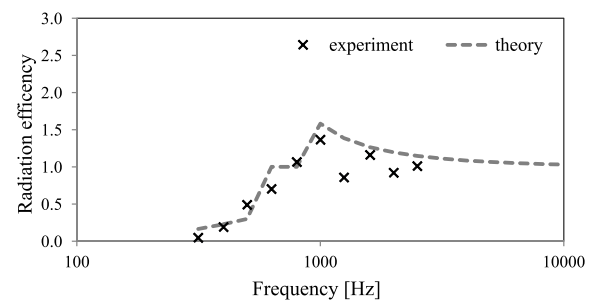


Fig. 9. Radiation efficiency of the cylinder.

From Table 7 and Fig. 9 one can infer the following:

- Theoretically estimated radiation efficiency shows a peak near ring frequency. This converges to unity at higher frequencies.
- The theoretically estimated radiation ratios are in good agreement with the experimental results except at 1250 Hz and 315 Hz. At low frequencies, the radiation resistance depends on the boundary conditions. Analytical formulation assumes simply supported boundary conditions while the experiment is conducted on a freely hung condition. This is probably the reason for the large difference seen at 315 Hz.
- Literature reported for acoustically thick shells (SZECHENYI, 1971; WANG, LAI, 2000) indicates that the radiation efficiency is unity beyond the critical frequency i.e. from 495 Hz in this case. This implies that there is no peak in the radiation efficiency at the ring frequency for acoustically thick category of cylinders. However, the analytical estimates as well the experimental results clearly indicate that there is significant sound radiation above critical frequency and it has a peak near its ring frequency.
- In the works reported so far (SZECHENYI, 1971; WANG, LAI, 2000), the radiation efficiency is considered to be unity at frequencies below the

ring frequency but above the critical frequency. Present results show that in this frequency range the radiation efficiencies can be less than unity. This is because in the above frequency range all the modes are not acoustically fast but only some of the modes are acoustically fast. The experimental results also show that the radiation efficiency in the above frequency range is less than unity.

- An expression for estimating the ring frequency of a composite cylinder is derived based on the speed of the in plane waves in composite plates. The ring frequency estimated using this expression is found to be close to experimentally observed ring frequency.

## 6. Conclusions

Sound radiation characteristics of an acoustically thick composite cylinder are determined through a numerical method and compared with the experimental results. While determining the structural wavenumbers the transverse shear deformation is also considered which is otherwise not considered before. In the absence of these results what is being practiced is that the radiation efficiency is considered as unity from critical frequency and beyond. It is shown that the radiation efficiency is lower than unity at frequencies between the critical and ring frequency and the sound radiation is quite significant near the ring frequency and beyond. Sound radiation characteristics of the cylinder are also determined through experiments. They are obtained from the measured sound pressure levels in a reverberation chamber for known velocities generated through mechanical excitation. The measured radiation characteristics are in very good agreement with the theoretically estimated results. From the speed of the in plane waves in composites, an expression for determining the ring frequency of composite cylinder is also derived. The experimental results are in agreement with the frequency obtained using the expression derived. The present investigation gives a very good insight in to the radiation characteristics of acoustically thick composite cylinders.

## Acknowledgement

Authors acknowledge the support rendered by Sameer Deshpande, S. Kesavan & Meenakshi Sundaram of Structures Group, URSC and Mr. Chandra of National Aerospace Laboratories during the course of this work. We express our sincere thanks to all the staffs of acoustic test facility, URSC for their kind help during the phase of the experimental work.

## References

1. BORDONI P.G., GROSS W. (1948), Sound radiation from a finite cylinder, *Journal of Mathematics and Physics*, **27**(1–4): 242–252, doi: 10.1002/sapm.1948271241.
2. BURROUGHS C.B. (1984), Acoustic radiation from fluid-loaded infinite circular cylinders with doubly periodic ring supports, *The Journal of the Acoustical Society of the America*, **75**(3): 715–722, doi: 10.1121/1.390582.
3. CAO X., HUA H., MA C. (2012), Acoustic radiation from shear deformable stiffened laminated cylindrical shells, *Journal of Sound and Vibration*, **331**(3): 651–670, doi: 10.1016/j.jsv.2011.10.006.
4. COX T.J., D’ANTONIO P. (2004), *Acoustic Absorbers and Diffusers: Theory, Design and Application*, New York: CRC Press.
5. FAHY F.J. (1969), Vibration of containing structure by sound in the contained fluid, *Journal of Sound and Vibration*, **10**(3): 490–512, doi: 10.1016/0022-460x(69)90228-4.
6. FAHY F.J. (1970), Response of a cylinder to random sound in the contained fluid, *Journal of Sound and Vibration*, **13**(2): 171–194, doi: 10.1016/s0022-460x(70)81172-5.
7. FYFE K.R., ISMAIL F. (1989), An investigation of the acoustic properties of vibrating finite cylinders, *Journal of Sound and Vibration*, **128**(3): 361–375, doi: 10.1016/0022-460x(89)90780-3.
8. GHINET S., ATALLA N., OSMAN H. (2006), Diffuse field transmission into infinite sandwich composite and laminate composite cylinders, *Journal of Sound and Vibration*, **289**(4–5): 745–778, doi: 10.1016/j.jsv.2005.02.028.
9. JOSEPHINE KELVINA FLORENCE S., RENJI K., SUBRAMANIAN K. (2018), Modal density of honeycomb sandwich composite cylindrical shells considering transverse shear deformation, *International Journal of Acoustics and Vibration*, **23**(3): 83–92, doi: 10.20855/ijav.2018.23.11241.
10. LAULAGNET B., GUYADER J.L. (1989), Modal analysis of a shell’s acoustic radiation in light and heavy fluids, *Journal of Sound and Vibration*, **131**(3): 397–415, doi: 10.1016/0022-460x(89)91001-8.
11. LE BOT A., COTONI V. (2010), Validity diagrams of statistical energy analysis, *Journal of Sound and Vibration*, **329**(2): 221–235, doi: 10.1016/j.jsv.2009.09.008.
12. LIN T.R., MECHEFSKE C., O’SHEA P. (2011), Characteristics of modal sound radiation of finite cylindrical shells, *Journal of Vibration and Acoustics*, **133**(5): 051011–051016, doi: 10.1115/1.4003944.
13. LYON R.H. (1975), *Statistical Energy Analysis of Dynamical Systems: Theory and Applications*, Cambridge, MA: MIT Press.
14. MANNING J.E., MAIDANIK G. (1964), Radiation properties of cylindrical shells, *The Journal of the Acoustical Society of the America*, **36**(9): 1691–1698, doi: 10.1121/1.1919266.
15. MILLER V.J., FAULKNER L.L. (1983), Prediction of aircraft interior noise using the statistical energy analysis.

- sis method, *Journal of Vibration, Acoustics, Stress and Reliability in Design*, **105**(4): 512–518, doi: 10.1115/1.3269136.
16. NORTON M.P. (1989), *Fundamentals of Noise and Vibration Analysis for Engineers*, England: Cambridge University Press.
17. QIAO Y., CHEN H.B., LUO J.L. (2013), Estimation of shell radiation efficiency using a FEM-SmEdA algorithm, *Journal of Vibroengineering*, **15**(3): 1130–1146.
18. RAMACHANDRAN P., NARAYANAN S. (2007), Evaluation of modal density, radiation efficiency and acoustic response of longitudinally stiffened cylindrical shell, *Journal of Sound and Vibration*, **304**(1–2): 154–174, doi: 10.1016/j.jsv.2007.02.020.
19. RENJI K., JOSEPHINE KELVINA FLORENCE S. (2020), Critical frequencies of composite cylindrical Shells, *International Journal of Acoustics and Vibration*, **25**(1): 79–87, doi: 10.20855/ijav.2020.25.11572.
20. RENJI K., JOSEPHINE KELVINA FLORENCE S., SAMEER DESHPANDE (2019), Characteristics of in-plane waves in composite plates, *International Journal of Acoustics and Vibration*, **24**(3): 458–466, doi: 10.20855/ijav.2019.24.31290.
21. RENJI K., JOSEPHINE KELVINA FLORENCE S., SAMEER DESHPANDE (2020), An Experimental investigation of modal densities of composite honeycomb sandwich cylindrical shells, *International Journal of Acoustics and Vibration*, **25**(1): 112–120, doi: 10.20855/ijav.2020.25.11626.
22. RENJI K., NAIR P.S., NARAYANAN S. (1998), On acoustic radiation resistance of plates, *Journal of Sound and Vibration*, **212**(4): 583–598, doi: 10.1006/jsvi.1997.1438.
23. REYNOLDS D.D. (1981), *Engineering Principles of Acoustics Noise and Vibration*, Boston, MA: Allyn and Bacon.
24. RUNKLE C.J., HART F.D. (1969), *The Radiation Resistance of Cylindrical Shells*, NASA CR-1437.
25. SQUICCIARINI G., PUTRA A., THOMPSON D.J., ZHANG X., SALIM M.A. (2015), Use of a reciprocity technique to measure the radiation efficiency of a vibrating structure, *Applied Acoustics*, **89**: 107–121, doi: 10.1016/j.apacoust.2014.09.013.
26. STEPHANISHEN P.R. (1978), Radiated power and radiation loading of cylindrical surfaces with non-uniform velocity distribution, *The Journal of the Acoustical Society of the America*, **63**(2): 328–338, doi: 10.1121/1.381743.
27. SUN Y., YANG T., CHEN Y. (2018), Sound radiation modes of cylindrical surfaces and their application to vibro-acoustics analysis of cylindrical shells, *Journal of Sound and Vibration*, **424**: 64–77, doi: 10.1016/j.jsv.2018.03.004.
28. SZECHENYI E. (1971), Modal densities and radiation efficiencies of unstiffened cylinders using statistical methods, *Journal of Sound and Vibration*, **19**(1): 65–81, doi: 10.1016/0022-460x(71)90423-8.
29. WANG C., LAI J.C.S. (2000), The sound radiation efficiency of finite length acoustically thick circular cylindrical shells under mechanical excitation. I: Theoretical analysis, *Journal of Sound and Vibration*, **232**(2): 431–447, doi: 10.1006/jsvi.1999.2749.
30. WANG C., LAI J.C.S. (2001), The sound radiation efficiency of finite length circular cylindrical shells under mechanical excitation II: Limitations of the infinite length model, *Journal of Sound and Vibration*, **241**(5): 825–838, doi: /10.1006/jsvi.2000.3338.
31. YIN X.W., LIU L.J., HUA H.X., SHEN R.Y. (2009), Acoustic radiation from an infinite laminate composite cylindrical shells with doubly periodic rings, *Journal of Vibration and Acoustics*, **131**(1): 011005–011009, doi: 10.1115/1.2980376.
32. ZHAO X., ZHANG B., LI Y. (2015), Vibration and acoustic radiation of an orthotropic composite cylindrical shell in a hygroscopic environment, *Journal of Vibration and Control*, **23**(4): 673–692, doi: 10.1177/1077546315581943.